

TAUP-2524-98  
M/C-TH-98/15

## Two Photon Reactions at High Energies

A. Donnachie

Department of Physics and Astronomy  
University of Manchester, Manchester M13 9PL, United Kingdom  
email: `ad@a3.ph.man.ac.uk`

H.G. Dosch

Institut für Theoretische Physik der Universität Heidelberg  
Philosophenweg 16, D-69120 Heidelberg, Germany  
email: `h.g.dosch@thphys.uni-heidelberg.de`

M. Rueter<sup>1</sup>

School of Physics and Astronomy  
Department of High Energy Physics, Tel Aviv University  
69978 Tel Aviv, Israel  
email: `rueter@post.tau.ac.il`

### Abstract

Cross sections for the reactions  $\gamma^{(*)}\gamma^{(*)} \rightarrow \text{hadrons}$  and  $\gamma^{(*)}\gamma^{(*)} \rightarrow 2 \text{ vector mesons}$  are calculated as functions of energy ( $\sqrt{s} \geq 20 \text{ GeV}$ ) and photon virtualities. Good agreement with experiment is obtained for the total hadronic cross section and, after allowing for a valence-quark contribution from the hadronic part of the photon, with the photon structure function at small  $x$ . The cross section for vector meson production are shown to be experimentally accessible for moderate values of  $Q^2$ . This is sufficient to probe the nature of the hard pomeron which has recently been proposed.

---

<sup>1</sup>Supported by a MINERVA-fellowship

# 1 Introduction

In the colour-dipole picture of high-energy scattering the scattering amplitude is expressed as a superposition of dipole-proton [1] or dipole-dipole [2] amplitudes. In the model of the stochastic vacuum [3, 4] as applied to high-energy scattering [2, 5, 6, 7] the dipole-dipole scattering amplitude is realized as the vacuum expectation value of two Wegner-Wilson loops. Any hadronic (or photonic) scattering amplitude can be expressed in terms of these amplitudes and the transverse wave functions of the hadrons (or photons) involved. Thus the model correlates a wide range of phenomena: hadron-hadron scattering [6, 7], vector meson electro- and photoproduction [8, 9] and deep inelastic scattering [10]. This is of considerable relevance as understanding the details of high-energy scattering at the microscopic level requires the investigation of many different processes within the context of a unified description.

The relevance of the dipole approach to deep inelastic scattering was first stressed by Nikolaev and Zakharov [1] and subsequently elaborated in a number of papers [11]. More recently the dipole-proton cross section  $\sigma_T(s, R_D)$  has been obtained from electroproduction data [12] as a function of energy and the dipole radius  $R_D$ . The data span dipole radii from 0.2 to 1.1 fm, and the cross section changes by more than an order of magnitude across this range. The model of the stochastic vacuum applied to high energy scattering is in reasonable accord with these results [13].

In this paper we investigate high-energy  $\gamma^{(*)}\gamma^{(*)}$  reactions. We calculate and predict the total real  $\gamma\gamma$  cross section, the real photon structure function at small  $x$  and reactions of the type

$$\gamma^{(*)}\gamma^{(*)} \rightarrow V_1 V_2, \quad (1)$$

where  $V_1$  and  $V_2$  can be any two vector mesons. These may be light quarkonia i.e.  $\rho$ ,  $\omega$ ,  $\phi$  or heavy quarkonia for which we restrict consideration to  $J/\psi$ .

The physics interest in these latter processes is that they are the closest one can get to the ideal of onium-onium scattering [14]. They provide as direct a measurement as is possible of colour dipole-dipole scattering, and the size of the dipoles can be tuned by the choice of vector meson or by the photon virtuality or both. The  $\gamma^{(*)}\gamma^{(*)}$  reactions have a considerable advantage over  $\gamma^{(*)}p$  reactions as the dipole scattering is measured directly and the complications arising from a proton target are avoided.

The ultimate goal is that the relevant experiments are performed to confirm the dipole approach and hence to obtain the dipole-dipole cross sections

$\sigma_T(s, R_{D_1}, R_{D_2})$  independently of specific theoretical models for a range of dipole radii  $R_{D_1}, R_{D_2}$ . At present one has to make use of specific models to provide an estimate of the cross sections. Our calculations demonstrate that significant measurements can be made with existing energies and luminosities. The present calculations are based on the fusion of two models. The absolute size and the dependence of the  $\gamma^{(*)}\gamma^{(*)}$  cross sections on the photon virtuality  $Q^2$ , and where relevant the choice of vector meson, are given by the model of the stochastic vacuum [3, 4] applied to high-energy scattering [5, 6] at a center of mass energy of about 20 GeV. This model can say nothing about the energy dependence, which is taken to be given by a two-pomeron model proposed recently [15] and which has subsequently been applied to the model of the stochastic vacuum [10].

The relevant aspects of these models are discussed in Section 2. In Section 3 we show that the model is in good agreement with data on the total hadronic  $\gamma\gamma$  cross section  $\sigma_{\gamma\gamma}$ , and we make predictions for the photon structure function  $F_2^\gamma(x, Q^2)$  at very small  $x$  and over a wide range of  $Q^2$ . At the higher values of  $x$  where data exist, combining our model with the VMD contribution corresponding to non-pomeron Regge exchange provides fair agreement with these data. Section 4 deals with the  $\gamma^{(*)}\gamma^{(*)} \rightarrow V_1 V_2$  cross sections in detail, and conclusions are drawn in Section 5.

## 2 The Model

The model of the stochastic vacuum (MSV) [3, 4] is based on the assumption that the infrared behaviour of QCD can be approximated by a Gaussian (i.e. factorizable) stochastic process in the gluon field strength tensor. With this simple assumption one obtains in non-Abelian gauge theories the area law for the Wegner-Wilson loop and hence confinement. Applying the model to the formalism for quark-quark scattering in the fempto-universe developed in [5] one can express any hadronic diffractive scattering amplitude in terms of a colour dipole-dipole scattering amplitude and the transverse wave functions of the hadrons (or photons) involved [2, 6].

We follow the notation and normalisation of [16]. The scattering matrix element for the reaction  $h_1 + h_2 \rightarrow h_3 + h_4$  is expressed in the form

$$\begin{aligned}
T = & 2is \frac{1}{4\pi} \int d^2 R_1 dz_1 \frac{1}{4\pi} \int d^2 R_2 dz_2 \int d^2 b e^{-i\vec{b}\vec{\Delta}} \tilde{J}(b, \vec{R}_1, z_1, \vec{R}_2, z_2) \\
& \times \psi_{h3}^*(\vec{R}_1, z_1) \psi_{h1}(\vec{R}_1, z_1) \psi_{h4}^*(\vec{R}_2, z_2) \psi_{h2}(\vec{R}_2, z_2).
\end{aligned} \tag{2}$$

Here  $\psi(\vec{R}_i, z_i)$  denotes the light-cone wave function of the hadron  $i$  or the

hadronic wave function of a photon,  $\vec{R}$  is the transverse extension,  $z$  is the fraction of longitudinal momentum,  $\vec{b}$  is the impact parameter,  $\vec{\Delta}^2 = t$  is the momentum transfer and  $\tilde{J}$  is given by eqn.(8) of [16]. For a discussion of these wave functions we refer to [9, 17].

We outline briefly the philosophy behind the choice of the photon wave function [17]. It is essentially given by the lowest-order perturbative expression for the quark-antiquark content of the photon, with chiral symmetry breaking and confinement being simulated by a  $Q^2$ -dependent quark mass. This procedure works remarkably well in quantum-mechanical examples. The quark mass was determined by comparing the zeroth-order result for the vector-current correlator with the analytically continued phenomenological expression ( $\rho$ -pole plus continuum) in the Euclidean region. The resulting mass is given by

$$\begin{aligned} m_{u,d} &= \begin{cases} m_0 (1 - Q^2/1.05) & : Q^2 \leq 1.05 \\ 0 & : Q^2 \geq 1.05 \end{cases} \\ m_s &= \begin{cases} 0.15 + 0.16 (1 - Q^2/1.6) & : Q^2 \leq 1.6 \\ 0.15 & : Q^2 \geq 1.6 \end{cases} \\ m_c &= 1.3. \end{aligned} \tag{3}$$

The parameter  $m_0$  for the  $u, d$  quarks was found to be  $\sim 0.22$  GeV.

A shortcoming of the stochastic vacuum model applied to high energy scattering is that it contains no explicit energy dependence. As a consequence most of the early applications were restricted to a center of mass energy of 20 GeV. However it is not difficult to insert an *ad hoc* energy dependence, and this is the procedure we adopt here.

The phenomenological soft pomeron of hadronic interactions cannot explain deep inelastic scattering or  $J/\psi$  photoproduction. A much stronger energy dependence is observed, and it varies with  $Q^2$ . In terms of an effective trajectory the latter fact implies a  $Q^2$  dependent intercept [18], in conflict with Regge theory. The suggestion [19] that there is a significant amount of shadowing in soft processes, which disappears at large  $Q^2$ , so that the observed effective intercept of  $\sim 1.08$  is the result of the pomeron having a much larger intercept is difficult to sustain. All soft processes are found to have the same value [20], and explicit model calculations [21] show that the  $p\bar{p}$  total and differential cross sections restrict the maximum value of the bare intercept to a much smaller value than is required by the deep inelastic and  $J/\psi$  data.

Consequently a two-pomeron model [15] has been proposed, based on a strict application of the Regge-pole formalism to such processes. Diffractive

processes are described by the exchange of *two* trajectories carrying vacuum quantum numbers with different *fixed* intercepts and with *residues* dependent on  $Q^2$ . The latter does not conflict with Regge theory. One of these trajectories is the conventional non-perturbative soft pomeron with an intercept  $\alpha_{soft} \sim 1.08$  whose residue is large for hadrons and photons with low  $Q^2$ , and a hard pomeron with an intercept  $\alpha_{hard} \sim 1.40$ . Before the problems associated with next-to-leading order contributions to the BFKL pomeron [22], it would have been tempting to identify this hard pomeron with the latter, but at present it is simply taken as a phenomenological prescription to describe the experimental data in a self-consistent way.

In a recent paper [10] the two pomeron approach scattering of [15] was extended to dipole-dipole scattering. All dipole-dipole amplitudes where both dipoles are larger than the value  $c = 0.35$  fm are multiplied by the energy dependent factor:  $(W^2/W_0^2)^{\alpha_{soft}(t)-1}$  with  $W_0 = 20$  GeV,  $\alpha_{soft}(t) = 1.08 + 0.25t$ . If one or both dipoles are smaller than  $c$  then the trajectory is replaced by the fixed pole  $\alpha_{hard} = 1.28$ . This value of  $\alpha_{hard}$  was chosen as experimentally  $F_2 \propto W^{0.56}$  at  $Q^2 = 20$  GeV<sup>2</sup> and the fixed-pole approximation made because of the lack of shrinkage in the  $J/\psi$  photoproduction differential cross section. It turns out that the model of the stochastic vacuum, which is supposed to be an approximation to the IR behaviour of QCD, overestimates the non-perturbative contributions of very small dipoles. Therefore the non-perturbative contribution is put to zero if one of the dipoles is smaller than some value  $r_{cut}$ , which came out as 0.16 fm. A diffractive scattering amplitude of a (virtual) photon with a hadron in this model is then given by the general expression

$$T(W^2, Q^2, t) = \beta_{soft}(Q^2, t)(W^2)^{\alpha_{soft}(t)} + \beta_{hard}(Q^2, t)(W^2)^{\alpha_{hard}(t)}. \quad (4)$$

For transverse photons of high virtuality  $Q^2$  another source of energy dependence is induced by the model. Since the hadronic size of the photon is determined by  $1/\sqrt{z(1-z)Q^2}$ ,  $z$  being the longitudinal momentum fraction, there will be at high values of  $Q^2$  a large contribution from quarks with very small longitudinal momentum  $zW/2$  or  $(1-z)W/2$ . The basis of the model is however that the momentum of the quarks should be large as compared to the Fourier components of the vacuum fluctuations. Therefore in [10] a cutoff for  $z$  (and  $1-z$ ) was introduced by requiring that  $zW \geq 0.2$  GeV,  $(1-z)W \geq 0.2$  GeV. This cutoff induces an additional energy dependence at presently accessible energies. Therefore the intercept of [10] is smaller than that of [15]. By simple Ansätze involving only four parameters it was possible to obtain in this way a good description of data for the proton structure function and electroproduction of vector mesons, without noticeably affecting

the earlier fits to hadron-hadron scattering. An interesting and relevant consequence of the model is that the total hadronic cross section for real photons has a stronger energy dependence than for purely hadronic scattering as the hard pomeron does not decouple in the limit  $Q^2 \rightarrow 0$ . This is a direct result of the hard component in the photon wave function. It is also a feature of the two-pomeron model of [15].

The advantage of relating the pomeron-coupling to dipoles (see also [11]) rather than to hadrons is twofold. First the dipole cross sections can be calculated directly in the MSV. Secondly once the coupling scheme is fixed the pomeron residues are determined by the corresponding wave functions. Thus in principle in the following predictions of the  $\gamma\gamma$  reactions there is *no new free parameter* involved. However the results for the  $\gamma\gamma$  total cross section depend strongly on the quark mass whereas the reactions we considered previously were quite insensitive to these parameters. So we allowed for small changes in the quark mass to obtain the right absolute size of the  $\gamma\gamma$  total cross section. Because of their insensitivity to this parameter these changes do not significantly affect any of our previous results.

### 3 $\gamma\gamma$ and $\gamma^*\gamma$ Scattering

Before making predictions for the  $\gamma^{(*)}\gamma^{(*)} \rightarrow V_1 V_2$  reactions, for which there is currently no high energy data, we show that the formalism predicts correctly the high energy data which do exist, namely the total hadronic  $\gamma\gamma$  cross section and the photon structure function. In both cases we restrict ourselves to comparison with the LEP data, as in the former case the photon energy is sufficiently high, and in the latter case the values of  $x_{Bj}$  are sufficiently small, for our model to be applicable.

#### 3.1 The Total Hadronic $\gamma\gamma$ Cross Section

The total hadronic  $\gamma\gamma$  cross section  $\sigma_{\gamma\gamma}$  has been measured recently at LEP by L3 [23] and by OPAL [24] for  $\gamma\gamma$  center of mass energies between 5 and 110 GeV. There is a small normalization difference between the two experiments, but both agree on the energy dependence which appears stronger than that observed in purely hadronic interactions. Interpreted in terms of a single pole, the effective intercept is  $1.158 \pm 0.006 \pm 0.028$  [23].

As already discussed the normalisation of  $\sigma_{\gamma\gamma}$  is very sensitive to the quark mass parameter  $m_0$ . In fact it varies as  $\sim 1/m_0^4$ . However the energy

dependence is not very sensitive to  $m_0$ . The predictions of our model for the the total  $\gamma\gamma$  cross section for  $m_0 = 220, 210$  and  $200$  MeV are shown in Fig.1. The energy dependence changes very little across this range of  $m_0$ , the effective intercept being 1.142, 1.145, 1.149 respectively for the three values. This energy dependence is a direct consequence of the hard pomeron not decoupling in the  $Q^2 \rightarrow 0$  limit of the proton structure function. Here the effect is more marked as the suppression of the hard component arising from the coupling to the proton is removed.

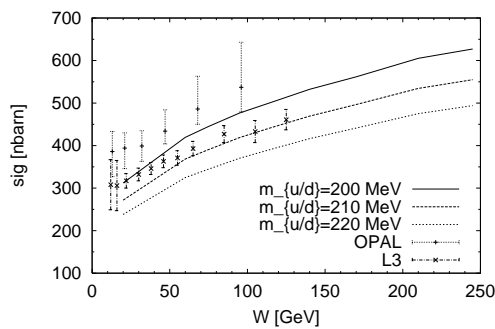


Figure 1: Preliminary experimental data for the total hadronic  $\gamma\gamma$  cross section from L3 [23] and OPAL [24] and our predictions for different values of the effective quark mass  $m_0$  (see eqn.(3)). The values of  $m_0$  are 220 MeV, 210 MeV and 200 MeV.

A choice of 210 MeV is clearly to be preferred to the initial value of 220 MeV of our previous publications, and we use 210 MeV throughout. This minor change has no effect on any of the purely hadronic predictions of the model and actually serves to improve slightly the description of high energy photon-proton reactions [17, 9]. Our curves fall below the data at smaller values of  $W$  because the non-pomeron Regge contribution, which we have not included, becomes important there.

### 3.2 The Photon Structure Function

The photon structure function  $F_2^\gamma(x, Q^2)$  has been measured over a wide range of  $Q^2$ , but primarily at rather large  $x$ . This restriction has been due to the machine energies previously available, but at LEP  $F_2^\gamma$  can be measured in the range  $x > 10^{-3}$  and  $1 < Q^2 < 10^3$  GeV<sup>2</sup> [25]. These measurements are in the domain where we expect pomeron dominance, and hence where our model can make specific predictions. Note that the two-pomeron model does not factorize simply, so that relating the photon structure function to

the proton structure function  $F_2^p$  by [26]

$$F_2^\gamma = F_2^p \frac{\sigma_{\gamma p}(W^2)}{\sigma_{pp}(W^2)} \quad (5)$$

is not valid. Obviously it is extremely important to check just how well simple factorization does hold. Note that the contribution from the valence quark structure function due to the hadronic content of the real photon will mask factorization, should it be valid, except at very small values of  $x$ .

A reasonable lower limit on the hadronic center-of-mass energy  $W$  for the application of the model is 15 GeV, which we convert to an upper limit on  $x$  for each  $Q^2$ . It turns out that this is more-or-less matched to the lower limit on  $x$  for which published data exist, which provides a check on the normalization, at least in principle. However the data are at values of  $x$  at which the valence quarks from the hadronic component of the photon contribute, and an estimate has to be made of this. Our direct predictions for the photon structure function, together with the data, are shown in Fig.2 by the dashed line. These are parameter free predictions and determine the photon structure function at small  $x$ . In view of possible forthcoming LEP data we have extended the calculations to values of  $x$  beyond those for which data are currently available.

As anticipated, our predictions are low in the region of overlap with current data as there is still a significant contribution from the valence quark structure function of the hadronic content of the real photon ( $\rho$ ,  $\omega$ ,  $\phi$  etc.) [29, 28, 27]. In naive vector meson dominance (VMD) this is given by

$$\frac{1}{\alpha} F_{2,had}^\gamma(x, Q^2) = F_{val}^\pi(x, Q^2) \sum_V \frac{4\pi}{f_V^2}, \quad (6)$$

where the sum is usually over  $\rho$ ,  $\omega$ ,  $\phi$ . The additional assumption has been made that the vector meson structure functions can all be represented by the valence structure function of the pion  $F_{val}^\pi(x, Q^2)$ . This in itself is quite an extreme statement, as there is no obvious reason why the structure function of the short-lived vector mesons should be the same as those of the long-lived pion. Additionally it is not clear whether one should take the simple incoherent sum or allow for coherence effects. Finally, higher mass vector mesons must also make some contribution, but this is almost certainly small compared to the uncertainties in any estimate of the hadronic component.

To add to these uncertainties, the pion structure function is only known experimentally for  $x > 0.2$ . To obtain the structure function in the kinematical domain of interest here, it is necessary to use the DGLAP evolution



equations to fit the data and to extrapolate [30, 31]. This was the approach used in fitting  $F_2^\gamma$  by [28, 27], although with somewhat different assumptions about the effective strength of the contribution. In contrast, in [29] the *shape* of the hadronic contribution was left free to be determined by the data, but the *normalization* was fixed.

For definiteness we have used the DGLAP evolved pion structure function of [28], and have retained only the  $\rho$ ,  $\omega$  and  $\phi$  in the sum of eqn.(6). Combining this with the predictions of our model for the singlet term gives a good description of the small- $x$  structure function. A comparison with the data of [32, 33, 34] is given in Fig.2.

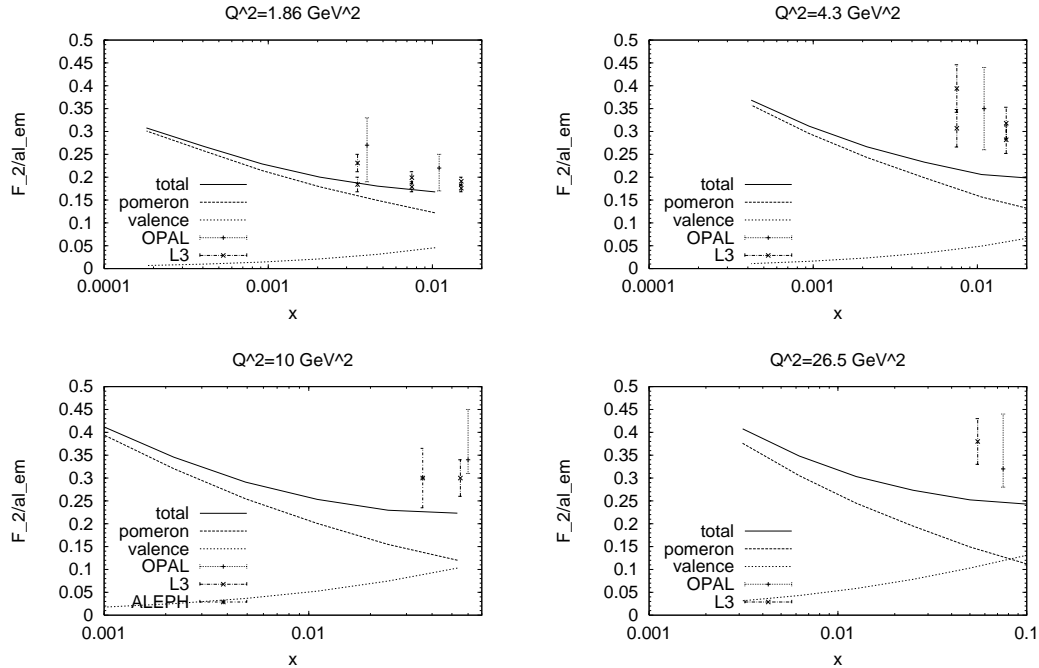


Figure 2: Data and predictions for the structure function  $F_2^\gamma/\alpha_{em}$  at small  $x$ . The data comprise preliminary data from Aleph [32] and L3 [33] and published data from OPAL [34]. The dashed line is the sea-quark (pomeron exchange) contribution, which dominates for small  $x$ , calculated in our approach without any free parameters. The dotted line is the estimated valence quark contribution (see text) and the solid line the sum of the two. The maximum  $x$ -value is chosen to give  $\sqrt{s} \geq 15$  GeV. The mean values of  $Q^2$  are 1.86 GeV<sup>2</sup>, 4.3 GeV<sup>2</sup>, 10.0 GeV<sup>2</sup> and 26.5 GeV<sup>2</sup>.

At smaller values of  $x$ , where pomeron exchange dominates and the valence quark contribution declines with increasing  $Q^2$ , our predictions for  $F_2^\gamma$

should be sufficient on their own. They agree rather well with the simple factorisation formula of eqn.(5) at small  $Q^2$ , but increasingly diverge as  $Q^2$  increases. This is not unexpected, as at small  $Q^2$  the proton structure function is dominated by a single term [15, 10] and factorization is a reasonable approximation. Interestingly at higher  $Q^2$  the predictions match well to those of [29], but lie below them at the lower values of  $Q^2$ .

#### 4 $\gamma^{(*)}\gamma^{(*)} \rightarrow V_1 V_2$

The model allows calculations to be performed for any vectors  $V_1, V_2$  in the light-quark or heavy-quark sectors, including radial excitations, and for any virtuality of the two photons. For simplicity we restrict ourselves to the following representative cases:  $\gamma^*(Q_1^2)\gamma^*(Q_2^2) \rightarrow \rho^0\rho^0$  for  $0 \leq Q_1^2 \leq 10 \text{ GeV}^2$ ,  $0 \leq Q_2^2 \leq 10 \text{ GeV}^2$ ,  $\gamma^*(Q_1^2)\gamma \rightarrow \rho^0\phi$  and  $\gamma^*(Q_1^2)\gamma \rightarrow \rho^0 J/\psi$  for  $Q_1^2 = 0$  and  $2.5 \text{ GeV}^2$  and  $\gamma\gamma \rightarrow J/\psi J/\psi$  for real photons. The latter is dominated by pomeron exchange at all energies and the former at sufficiently high energy. We note that the dominance of pomeron exchange can be assured in the light-quark sector at any energy by considering  $\gamma^{(*)}\gamma^{(*)} \rightarrow \phi\phi$  or  $\gamma^{(*)}\gamma^{(*)} \rightarrow \rho\phi$ , although the cross sections are obviously appreciably smaller than those for  $\rho\rho$  production.

The results for the  $\rho\rho$  total cross section are shown in Fig.3 as a function of the  $\gamma^*\gamma^*$  center-of-mass energy  $W$ , multiplied by the naive VMD factor  $(Q_1^2 + m_\rho^2)^2(Q_2^2 + m_\rho^2)^2$ . This is to provide a common scale, and to demonstrate quite explicitly that the cross sections do *not* follow simple VMD. That they do not is unsurprising. The effect of the hard pomeron contribution is explicitly *not* like VMD, and the  $Q^2$ -dependence is more intricate than simple VMD as it depends on the size of the dipole. The other notable difference is that the energy dependence changes with increasing  $Q^2$  as opposed to the  $Q^2$ -independent behaviour expected of simple VMD. The results show clearly the dominance of the soft pomeron for small photon virtuality and the increasing importance of the hard pomeron as the photon virtuality increases. The dominance of the hard pomeron term sets in much more rapidly than in  $\gamma^*p$  reactions. Its presence is already visible at  $Q^2 = 0$  and by  $Q^2 = 2.5 \text{ GeV}^2$  it is dominating the cross section.

The differential cross sections  $d\sigma/dt$  (*without* the VMD normalization factor) are shown in Fig.4 for the two extremes  $Q_1^2 = Q_2^2 = 0$  and  $Q_1^2 = Q_2^2 = 10 \text{ GeV}^2$ . Shrinkage, that is an energy dependence of the slope of  $d\sigma/dt$ , due to the Regge factor  $2\alpha'(t) \log s$  is clearly visible for the case of two real photons, emphasizing the dominant contribution from the soft pomeron.

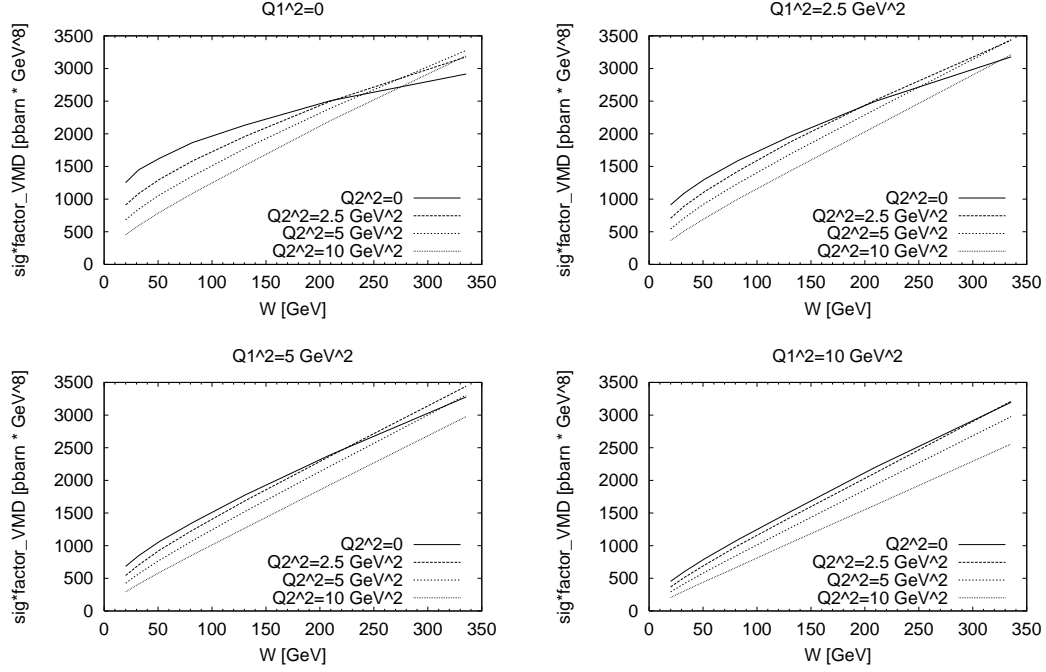


Figure 3: Predicted cross sections for the reaction  $\gamma^{(*)}\gamma^{(*)} \rightarrow \rho\rho$ . The virtuality of the first photon is  $Q_1^2 = 0 \text{ GeV}^2$ ,  $2.5 \text{ GeV}^2$ ,  $5.0 \text{ GeV}^2$  and  $10 \text{ GeV}^2$ . In each case the same virtualities are shown for the second photon. The cross sections have been scaled by the VMD factor  $(Q_1^2 + m_\rho^2)^2(Q_2^2 + m_\rho^2)^2$ .

Shrinkage is much less obvious for the case of large photon virtuality, where the hard pomeron is now the dominant contribution. Figure 4 also shows the decrease in cross section with increasing photon virtuality which is masked in Fig.3 by the VMD normalization factor.

In Fig.5 we show the cross sections for  $\gamma^*\gamma \rightarrow \rho\phi$  and  $\gamma^*\gamma \rightarrow \rho J/\psi$  to illustrate that even for quite modest photon virtuality on the  $\rho$  the hard pomeron dominates. The total cross section for  $\gamma\gamma \rightarrow J/\psi J/\psi$  is also shown in Fig.5. As it is already very small, we do not give any results for non-zero photon virtuality. In practice the measurable cross section will be much less as we have taken no account of the branching fraction of the  $J/\psi$  to  $\mu^+\mu^-$ . The almost complete dominance of the hard pomeron is obvious, and is more marked than for  $J/\psi$  photoproduction.

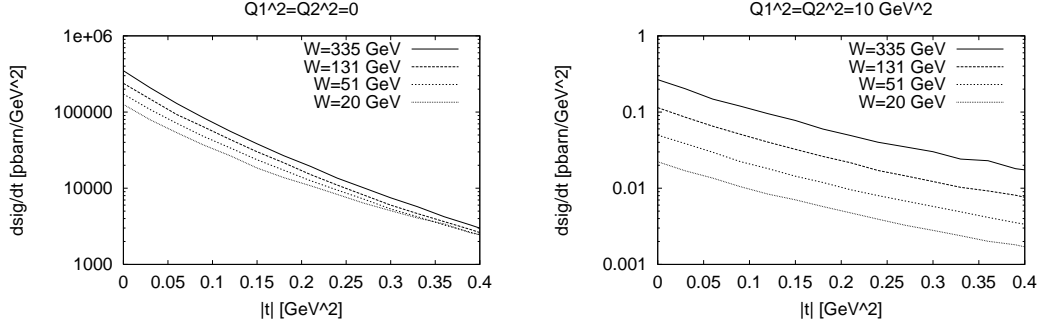


Figure 4: The differential cross section  $d\sigma/dt$  for  $\gamma\gamma \rightarrow \rho\rho$  for  $Q_1^2 = Q_2^2 = 0$  and  $Q_1^2 = Q_2^2 = 10 \text{ GeV}^2$ . These cross sections have *not* been scaled by a VMD factor.

## 5 Conclusions

We have demonstrated that the two-pomeron modification [10] of the MSV model correctly predicts the energy dependence of the  $\gamma\gamma$  total cross section without any adjustment of parameters. However to obtain the correct normalization it is necessary to change the quark mass to 210 MeV from the 220 MeV of our previous publications. This then gives good agreement for  $W > 50 \text{ GeV}$  where we can neglect the non-pomeron Regge contributions. Our results also agree with the photon structure function at small  $x$ , within the limitations of the present data and the uncertainties on the valence quark content of the hadronic component of the photon. This justifies the use of the model to estimate cross sections for  $\gamma^{(*)}\gamma^{(*)} \rightarrow V_1 V_2$ . These are found to be at a level which, in principle, allows a rather direct determination of the colour dipole-dipole cross section. Similar results for the case of purely real photons have been obtained recently in a rather different model [35]. We stress the importance of photon virtuality, even if small, in probing the most interesting part of high-energy scattering.

Apart from taking into account a hard pomeron our choice of the photon wave function is decisive for the results. The hard part of it leads to a non-negligible coupling of the hard pomeron even to the real photon, in contrast with purely hadronic reactions. This hard component, already present in the real photon, and the small value of the mass parameter  $m_0 = 210 \text{ MeV}$ , also explains why the hard contribution plays a decisive role even at moderate virtualities. We demonstrate these features graphically in Fig.6.

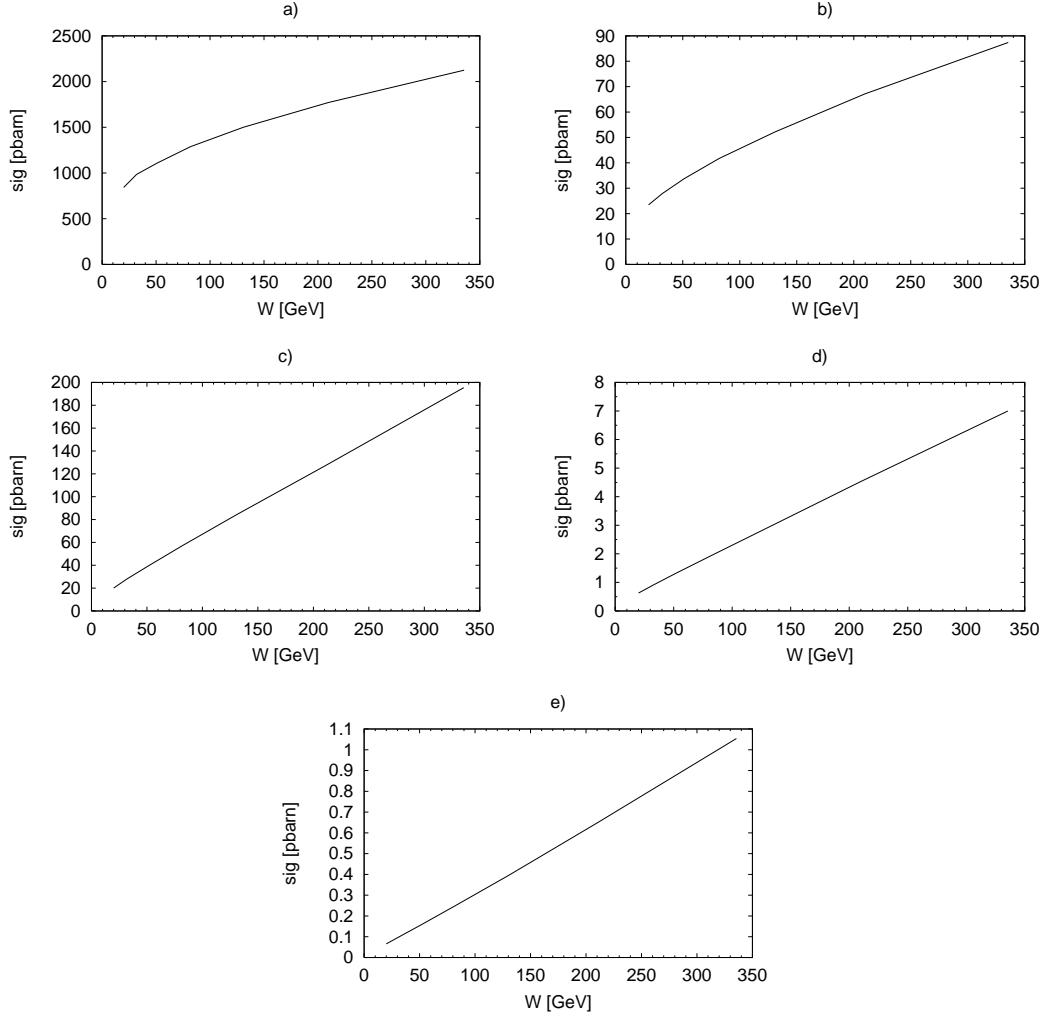


Figure 5: Total cross section of vector meson production in photon-photon scattering as a function of energy: a)  $\gamma\gamma \rightarrow \rho\phi$ , b)  $\gamma^*\gamma \rightarrow \rho\phi$  for  $Q_1^2 = 2.5 \text{ GeV}^2$ , c)  $\gamma\gamma \rightarrow \rho J/\psi$ , d)  $\gamma^*\gamma \rightarrow \rho J/\psi$  for  $Q_1^2 = 2.5 \text{ GeV}^2$  and e)  $\gamma\gamma \rightarrow J/\psi J/\psi$ .

## Acknowledgments

The authors thank Peter Landshoff and Otto Nachtmann for interesting discussions. One of us (A.D.) wants to thank the Institut für Theoretische Physik der Universität Heidelberg for the hospitality extended to him during his stay there and the Bundesministerium für Bildung, Wissenschaft, Forschung und Technologie for financial support. H.G.D. acknowledges sup-

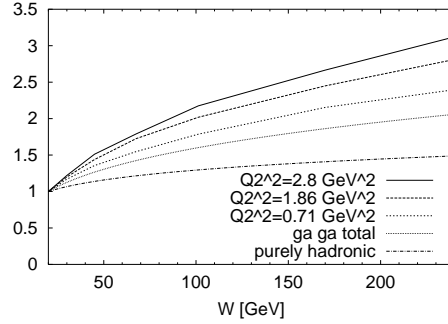


Figure 6: Comparison of the energy dependence of a typical purely hadronic total cross section, the  $\gamma\gamma$  total cross section and the  $\gamma\gamma^*$  total cross section for  $Q_2^2=0.71 \text{ GeV}^2$ ,  $1.86 \text{ GeV}^2$  and  $2.8 \text{ GeV}^2$  to illustrate how rapidly the hard pomeron term dominates in  $\gamma\gamma^*$  scattering. Because here we are only interested in the energy dependence we scaled all cross sections to the same value at  $W = 20 \text{ GeV}$ .

port from DAAD and M.R. is grateful to the MINERVA-Stiftung for financial support.

## References

- [1] N.N. Nikolaev and B.G. Zacharov: Z.Phys. **C49** (1991) 607
- [2] A. Krämer and H.G. Dosch: Phys.Lett. **B272** (1991) 114
- [3] H.G. Dosch: Phys.Lett. **B190** (1987) 555
- [4] H.G. Dosch and Yu.A. Simonov: Phys.Lett. **B205** (1988) 339
- [5] O. Nachtmann: Ann.Phys. **209** (1991) 436
- [6] H.G. Dosch, E. Ferreira and A. Krämer: Phys.Rev. **D50** (1994) 1992
- [7] E. Berger and O. Nachtmann: hep-ph/9808320, Eur.Phys.J. **C** (1999) DOI 10.1007/s100529801026
- [8] H.G. Dosch, T. Gousset, G. Kulzinger and H.J. Pirner: Phys.Rev. **D55** (1997) 2602
- [9] G. Kulzinger, H.G. Dosch and H.J. Pirner: hep-ph/9806352, Eur.Phys.J. **C** (1999) DOI 10.1007/s100529800986

- [10] M. Rueter: hep-ph/9807448, Eur.Phys.J. **C** (1999) DOI 10.1007/s100529801002
- [11] N.N. Nikolaev and B.G. Zakharov: Phys.Lett. **B327** (1994) 149; ibid 157  
J. Nemchik, N.N. Nikolaev and B.G. Zakharov: Phys.Lett. **B341** (1994) 228
- [12] J. Nemchik, N.N. Nikolaev, E. Predazzi and B.G. Zacharov: Phys.Lett. **B374** (1996) 199 and Z.Phys. **C75** (1997) 71
- [13] M. Rueter and H.G. Dosch: Phys.Rev. **D57** (1998) 4097
- [14] A.H. Mueller: Nucl.Phys. **B415** (1994) 373  
A.H. Mueller and H. Patel: Nucl.Phys. **B425** (1994) 471
- [15] A. Donnachie and P.V. Landshoff: Phys.Lett. **B437** (1998) 408
- [16] M. Rueter, H.G. Dosch and O.Nachtmann: hep-ph/9806342, Phys.Rev. **D59** (1999) 014018
- [17] H.G. Dosch, T. Gousset and H.J. Pirner: Phys.Rev. **D57** (1998) 1666
- [18] A. Capella, A. Kaidalov, C. Merino and J. tran Thanh Van: Phys.Lett. **B337** (1994) 358  
M. Bertini, M. Giffon and E. Predazzi: Phys.Lett. **B349** (1995) 561
- [19] E. Gotsman, E.M. Levin and U. Maor: Phys.Rev. **D49** (1994) 4321
- [20] Particle Data Group: Eur.Phys.J. **3** (1998) 205
- [21] S.V. Goloskokov, S.P. Kuleshov and O.V. Selyugin: hep-ph/9409383  
A. Donnachie: private communication
- [22] V.S. Fadin and L.N. Lipatov: Phys.Lett. **B429** (1998) 127
- [23] L3 Collaboration: M. Acciari et al: Phys.Lett. **B408** (1997) 450  
L3 Collaboration: *Cross section of hadron production in  $\gamma\gamma$  collisions at LEP*, talk at *XXIX ICHEP*, Vancouver, Canada, 1998
- [24] OPAL Collaboration: F. Wäckerle: talk at *XXVIII Int. Symp. on Multiparticle Dynamics*, Frascati, Italy, 1997
- [25] S. Söldner-Rembold: talk at *XVIII ISLEPHI*, Hamburg, Germany, 1997
- [26] H. Abramowicz, E. Gurvich and A. Levy: Phys.Lett. **B420** (1998) 104

- [27] P. Aurenche, M. Fontannaz and J.Ph. Guillet: Z.Phys. **C64** (1994) 621
- [28] M. Glück, E. Reya and A. Vogt: Phys.Rev. **D46** (1992) 1973
- [29] G.A. Schuler and T. Sjöstrand: Z.Phys. **C68** (1995) 607
- [30] P. Aurenche: Phys.Lett. **B233** (1989) 517
- [31] M. Glück, E. Reya and A. Vogt: Z.Phys. **C53** (1992) 651
- [32] Aleph Collaboration: *Measurement of the Photon Structure Function at  $Q^2$  of 8.9 and 19.1 GeV<sup>2</sup>*, talk at *XXIX ICHEP*, Vancouver, Canada, 1998
- [33] L3 Collaboration: CERN-EP/98-98 and *Study of the Hadronic Photon Structure Function  $F_2^\gamma$  at  $\sqrt{s} \sim 183$  GeV*, talk at *XXIX ICHEP*, Vancouver, Canada, 1998
- [34] OPAL Collaboration: Phys.Lett. **B411** (1997) 387 and Phys.Lett. **B412** (1997) 225
- [35] M.M. Block, E.M. Gregores, F. Halzen and G. Pancheri: hep-ph/9809403